

UDC 539.219.2: 548.73

<https://doi.org/10.17073/0021-3438-2023-4-48-59>

Research article

Научная статья



Sputtering by inverted magnetrons: influence on the texture and residual stresses in four layer Ta/W/Ta/W coatings

A.A. Lozovan, S.Ya. Betsofen, A.S. Lenkovets, A.V. Shalin, N.A. Ivanov

Moscow Aviation Institute (National Research University)

4 Volokolamskoe shosse, Moscow 125993, Russia

✉ Alexander A. Lozovan (loz-plasma@yandex.ru)

Abstract: The aim of the study is to examine the possibilities of sputtering of multilayer coatings at a high rate of deposition on products of complex shape using inverted magnetrons. The formation of texture and residual stresses in magnetron four-layer Ta/W/Ta/W coatings deposited at voltages from 0 to –200 V on cylindrical and flat copper substrates imitating elements of the surface of complex shape products was evaluated using the X-ray method of inverse pole figures and the $\sin^2\Psi$ method. The patterns of texture formation in coatings depend mainly on the bias voltage on the substrate (U_s), while at $U_s = -200$ V they differ for W and Ta layers. At $U_s = -100$ V, the epitaxial mechanism of texture formation is realized. In the case of a cylindrical substrate, this leads to intense texture (111) of all four layers. In the case of a flat substrate, this can lead to the formation of a single-crystal texture (111) in all layers with a texture maximum width of 12° – 14° . The presence of a single-crystal (111) tantalum texture corresponds to the maximum Young moduli and, accordingly, the interatomic bonding forces normal to the coating plane. This suggests that multilayer coatings with an external Ta layer have high tribological characteristics. Increasing the voltage on a flat substrate from 0 to –200 V leads to an increase in residual compressive stresses from 0.5 to 2.7 GPa for the four-layer coating under study.

Keywords: Ta/W/Ta/W coatings, « $\sin^2\Psi$ » method, texture, residual stresses, bias voltage.

Acknowledgements: This research was supported by the Russian Science Foundation (grant no. 22-19-00754).

For citation: Lozovan A.A., Betsofen S.Ya., Lenkovets A.S., Shalin A.V., Ivanov N.A. Sputtering by inverted magnetrons: influence on the texture and residual stresses in four layer Ta/W/Ta/W coatings. *Izvestiya. Non-Ferrous Metallurgy*. 2023;29(4):48–59.

<https://doi.org/10.17073/0021-3438-2023-4-35-59>

Исследование влияния условий напыления системой инвертированных магнетронов на текстуру и остаточные напряжения в четырехслойных Ta/W/Ta/W-покрытиях

А.А. Лозован, С.Я. Бецофен, А.С. Ленковец, А.В. Шалин, Н.А. Иванов

Московский авиационный институт (Национальный исследовательский университет)

125993, Россия, г. Москва, Волоколамское шоссе, 4

✉ Александр Александрович Лозован (loz-plasma@yandex.ru)

Аннотация: Исследованы возможности нанесения с высокой скоростью осаждения многослойных покрытий на изделия сложной формы с помощью инвертированных магнетронов. Рентгеновским методом обратных полюсных фигур и методом « $\sin^2\Psi$ » оценивали формирование текстуры и остаточных напряжений в магнетронных четырехслойных Ta/W/Ta/W-покрытиях, нане-

сенных при напряжениях от 0 до -200 В на цилиндрическую и плоскую подложки из меди, имитирующие элементы поверхности изделий сложной формы. Показано, что закономерности формирования текстуры в покрытиях зависят в основном от напряжения смещения на подложке (U_n), при этом при $U_n = -200$ В они отличаются для слоев W и Ta. При $U_n = -100$ В реализуется эпитаксиальный механизм текстурообразования, который в случае цилиндрической подложки приводит к интенсивной (111) текстуре всех четырех слоев, а в случае плоской – к формированию во всех слоях монокристалльной (111) текстуры с шириной текстурного максимума 12° – 14° . Наличие монокристалльной (111) текстуры тантала соответствует максимальным значениям модуля Юнга и, соответственно, сил межatomной связи нормально плоскости покрытия, что предполагает у многослойных покрытий с внешним Ta-слоем высокие трибологические характеристики. Увеличение напряжения на плоской подложке от 0 до -200 В приводит к повышению остаточных сжимающих напряжений от 0,5 до 2,7 ГПа для исследуемого четырехслойного покрытия.

Ключевые слова: Ta/W-Ta/W-покрытия, метод « $\sin^2\Psi$ », текстура, остаточные напряжения, напряжение смещения.

Благодарности: Работа выполнена при финансовой поддержке Российского научного фонда (грант № 22-19-00754).

Для цитирования: Лозован А.А., Бецофен С.Я., Ленковец А.С., Шалин А.В., Иванов Н.А. Исследование влияния условий напыления системой инвертированных магнетронов на текстуру и остаточные напряжения в четырехслойных Ta/W-Ta/W-покрытиях. *Известия вузов. Цветная металлургия*. 2023;29(4):48–59.

<https://doi.org/10.17073/0021-3438-2023-4-48-59>

Introduction

Refractory coatings, primarily based on tungsten, are promising for various applications such as: microelectronics [1], including spintronics [2; 3]; thermophotovoltaic converters in power engineering; and high-temperature nanophotonics [4]. They can be in demand as thermal barrier coatings for parts of future thermonuclear reactors such as ITER [5; 6], subject to extreme thermal stress and ion bombardment. They can also be used for other heat loaded products such as rocket engine combustion chambers. Key issues for such coatings are thermomechanical stability against delamination, tungsten oxide formation and diffusion at high operating temperatures, as well as the difficulty of achieving long-term high temperature stability in terms of preventing grain growth [4].

Tantalum coatings are of particular interest because they are a promising candidate for the replacement of electrolytic chrome coatings, often used in a variety of tribological and corrosion-resistant applications. Replacement of these coatings is justified, since chromium waste contains 6-valent chromium, a known carcinogen dangerous to the environment. Paper [7] presents the results of a study of the formation of thin magnetron films of α - and β -Ta. It shows that when applied to an amorphous substrate (α -Si, α -SiO_x, α -SiN_x), β -Ta is formed. This belongs to the spatial group of tetragonal syngony $P-4_2/m$ ($a = 10.194$ Å, $c = 5.313$ Å) with strong axial texture [001]. Heating of Ta coating to 176°C leads to the formation of α -Ta along with β -Ta, and at a temperature $> 326^\circ\text{C}$, a single-phase structure of α -Ta is formed. When such coatings are applied to crystalline molybdenum, α -Ta with a texture [110] is formed.

An important role for multilayer coatings is played by the texture of individual layers formed in them, since the efficiency of stress relaxation processes at the interface depends on this. In addition, texture is a defining characteristic for many service properties due to their pronounced orientational dependence. In this regard, special attention should be paid to Ta. Unlike W, it has a pronounced anisotropy of elastic and, with a high probability, also tribological properties. In [8], the phase composition, texture and residual stresses in magnetron Ta coatings of thickness (h) up to $40\ \mu\text{m}$ sputtered at $t = 20\div 400^\circ\text{C}$ were investigated. At room temperature β -Ta with (001) texture is formed; at $t = 300^\circ\text{C}$ — a two-phase mixture of β - and α -Ta with β -Ta dominating with (001) texture (while α -Ta has no pronounced texture); at $t = 400^\circ\text{C}$ — α -Ta with pronounced (110) texture.

The dependence of the α -Ta texture on the film thickness was found. At $h > 10\ \mu\text{m}$, the texture (110) is transferred to (111). The phase composition and texture change as the final coating thickness is formed.

In [9], an *in-situ* X-ray study of tantalum film growth during deposition using a planar magnetron at distances from the target to the glass substrate of 25 and 108 mm was carried out. In the first case, deposition was carried out at a rate of $6.4\ \text{nm/min}$, with an amorphous layer with a thickness of $45\ \text{nm}$ closest to the substrate, followed by a β -Ta layer with $h = 15\ \text{nm}$, and then an α -Ta layer with $h = 190\ \text{nm}$. In the second case, the deposition rate was $1.6\ \text{nm/min}$ and the amorphous layer occupied almost 90 % of the total film thickness of $36\ \text{nm}$. β -Ta

had texture (002) and α -Ta was characterized by texture (110), and the degree of texturing increased with the time of film deposition.

The authors [10] investigated the structure of Ta coatings deposited using magnetron sputtering at different bias voltages ranging from 0 to -100 V. This has a marked influence on the phase structure of these coatings. When the bias voltage was increased from 0 to -70 V, their structure changed from a single-phase β -phase at U_s from 0 to -20 V to a two-phase structure in the range of -30 to -40 V and to a full α -phase when the U_s values were in the range of -50 to -100 V. The authors managed to obtain a coating with a thickness of $100\text{ }\mu\text{m}$ with good mechanical properties and relatively low residual stresses (-2.1 GPa) for this thickness.

In [11], the influence of argon pressure (P_{Ar}) from 0.3 to 1.4 Pa on the phase composition, texture, residual stresses, and hardness of magnetron Ta coatings 10 – 1000 nm thick was investigated. At all P_{Ar} , the coatings consisted of a metastable β -phase, and only at 0.7 Pa was the α -phase Ta detected. For most coatings, compressive stresses from -200 to -1500 MPa were observed, but tensile stresses from 400 to 1100 MPa were found in a number of coatings. The hardness of the coatings varied from 10.2 to 17.7 GPa. At the same time, no correlations were found between hardness and texture or with the magnitude of residual stresses.

The authors of [12] considered the influence of the conditions for deposition of magnetron coatings by the modulated pulse method on the structure and properties of Ta coatings. Their phase composition depends on temperature. The α -Ta phase is formed at a substrate temperature above 365 – 375 °C, achieved in ~ 150 min. The β -Ta phase is formed at lower temperatures. For this reason, β -Ta is formed at the initial stage of coating formation, and only at a distance of $>14\text{ }\mu\text{m}$ from the substrate the α -Ta phase begins to dominate. Measurements of residual stresses in coatings 5 – $20\text{ }\mu\text{m}$ thick showed the presence of compressive stresses from -2.0 to -2.2 GPa for coatings with $h = 5, 8, 14$; and $20\text{ }\mu\text{m}$ and tensile stresses of 1.7 GPa only for coatings with $h = 6\text{ }\mu\text{m}$.

Composite multilayer W/Ta coatings with both a BCC structure and a close surface energy of 3.26 and 2.9 J/m^2 , respectively, have been intensively studied in order to establish their possible application in a variety of applied problems [13–15]. Important among them is the development of a method for applying a multilayer uniform thickness W/Ta-coating on the surface of products of complex shape.

Direct current planar magnetron sputtering (DCMS) and high-power pulsed magnetron sputtering (HP-PMS) have been successfully used [16] to deposit W/Ta. HPPMS coating is denser and has a smoother surface than DCMS which is a consequence of the deposition of a stream with a higher degree of ionization of the sputtered atoms [17]. However, from the point of view of industrial application, the main disadvantage of HPPMS technology is the significantly lower deposition rate compared to DCMS [16].

Simultaneously resolving both of these problems by using inverted strip magnetrons is also a relevant objective. [17] shows that hollow cathode deposition, in which the substrates are mounted on the axis of an elongated tubular source, can be an efficient method of coating complex-shaped objects. In a hollow cathode magnetron with a uniform current density and a cosine angular distribution of the sputtered material, the sputtered flux (per unit area) at all points inside the cathode (where the final effects are not important) is equal to the cathode erosion flux, regardless of the pressure of the working gas. The authors obtained a copper deposition rate of 400 nm/min . However, it should be borne in mind that when the substrate is large, and the space between it and the cathode becomes a thin ring, the geometry approaches a planar cathode and backscattering of the sputtered atoms reduces the deposition rate.

[18; 19] shows that in order to create thin-walled small-sized axisymmetric shell structures made of layered composites: for example, tubular products with different surface profiles; a system of successively arranged inverted field-cathode magnetrons; and one straight cylindrical magnetron used to clean the substrates is very efficient. Such a system allows the formation of layered composite shells by sputtering various layers onto a mandrel (for example, made of copper) which is subsequently etched.

The aim of achieving uniformity of the coating on the surface of products of complex shape cannot be isolated from the problem of structure, since the microstructure of coatings deposited in vacuum depends on the deposition rate, the directions of arrival of coating atoms, pressure of the working gas, as well as the ion bombardment flux, bias voltage (U_s) on the substrate and its temperature.

This work studies the formation of texture and residual stresses in individual layers of four-layer Ta/W/Ta/W coatings deposited by a system of inverted strip cathode magnetrons on copper substrates of various shapes (flat and cylindrical) at bias voltages on the substrate from 0 to -200 V.

Experimental

The sputtering deposition was carried out using a system of inverted magnetrons installed in series at a distance of 30 mm from each other on a specialized MRM-1 setup as presented in [18]. Argon with a purity of at least 99.9 % was selected as the working gas. The cathode material was W and Ta with a purity of ≈ 99.9 %; the inner diameter and length of the cathodes were 37 and 24 mm, respectively. A tube made of copper M-1 with a diameter of 10 mm and a length of 20 mm was used as a substrate. Before sputtering, the tube was polished and washed in an ultrasonic cleaner in acetone and alcohol. Then the substrate was installed on the rod for vertical movement of samples in the chamber and evacuated to a residual pressure of 10^{-3} Pa. Before sputtering, the glow discharge plasma treatment was applied for 30 min at argon pressure of 5 Pa and a voltage on the substrate of 1100 V. Next, deposition of tantalum and tungsten was carried out at different bias voltages on the substrate according to the regimes presented in Table 1. During sputtering, the substrate performed reciprocating movements along the cathode axis and periodically completely left the cathode area, both ends alternately. Each layer was deposited for 2 h, sputtering all samples for 8 h and obtaining a total coating thickness of 198, 189, 167, 128, and 64 μm at $U_s = 0, -50, -100, -150, \text{ and } -200$ V, respectively. The layers alternated in the Ta/W/Ta/W sequence.

The texture was estimated using quantitative inverse pole figures (IPF) by taking diffraction patterns in the angle range $2\theta = 30^\circ \div 140^\circ$ in filtered $\text{CuK}\alpha$ radiation. The pole density for 6 normals to (hkl) on a stereogra-

phic triangle (001, 011, 013, 111, 112, 123) was determined by the equation:

$$P_{(hkl)} = n \frac{I_{(hkl)} / R_{(hkl)}}{\sum_{i=1}^n (I_{(hkl)} / R_{(hkl)})}, \quad (1)$$

where $I_{(hkl)}$ and $R_{(hkl)}$ are the integral intensities of reflections (hkl) for texturized and textureless (reference) samples, respectively; $n = 6$ is the number of independent (hkl) reflections.

In diffraction strain measurement, the “ $\sin^2\Psi$ ” method is widely applied, in which the interplanar distances for reflection (hkl) are measured at several values of the tilt angle Ψ . The residual stress value is determined by the slope ($\text{tg}\alpha$) of the experimental dependence d_Ψ (interplanar distance at the slope angle Ψ) on $\sin^2\Psi$:

$$\sigma_{\text{ост}} = \frac{\text{tg}\alpha E_{(hkl)}}{d_0 (1 + \nu_{(hkl)})}, \quad (2)$$

where $E_{(hkl)}$ and $\nu_{(hkl)}$ are the Young's modulus and the Poisson's ratio for the direction of the normal to (hkl) ; d_0 is the interplanar distance at $\Psi = 0$.

Results and discussion

Investigation of texture in four-layer coating

Figures 1 and 2 show combined diffraction patterns of magnetron coatings Ta, Ta/W, Ta/W/Ta, and Ta/W/Ta/W deposited on a cylindrical Cu substrate at voltages $U_s = -100$ and -200 V. Analysis of these

Table 1. Sputtering regimes

Таблица 1. Режимы напыления

Regime	Layer	U_m, V	I_m, A	$-U_s, \text{V}$	I_s, A	P_{Ar}, Pa	$t, ^\circ\text{C}$
1	Ta	280–285	1	—	—	0.2	420
	W	290–305	1	—	—	0.2	430
	Ta	275–285	1	—	—	0.2	415
	W	290–305	1	—	—	0.2	430
2	Ta	270–280	1	50 (100, 150, 200)	0.14–0.05	0.2	430
	W	290–300	1	50 (100, 150, 200)	0.14–0.05	0.2	440
	Ta	270–285	1	50 (100, 150, 200)	0.14–0.05	0.2	430
	W	290–305	1	50 (100, 150, 200)	0.14–0.05	0.2	440

diffraction patterns, summarized in Fig. 3 as dependences of the pole densities of reflections (211), (321) and (222) for successive layers in four-layer coatings, indicates that the regularities of texture formation depend mainly on the stress on the substrate. However, they differ for W and Ta layers. This is especially noticeable for coatings deposited at $U_s = -200$ V (see Fig. 3, b).

The use of the calculation of pole densities gives a more adequate and, in addition, a quantitative picture of the features of texture formation in comparison with a qualitative consideration of the reflection intensities in diffractograms. The intensity of the reflection (222) in the textureless reference is 7 and 6 times less than the intensity of the reflections (321) and (211), respectively. In addition, the angular width of the reflection (222) is almost 2 times greater than the reflection (211). Therefore, at the same height of both reflections (211) and the pole density (222) is more than an order of magnitude higher, observed in Fig. 3, a.

The influence of the bias voltage on the substrate on texture formation in a four-layer coating can be seen in the fact that at $U_s = -100$ V (Fig. 3, a) an epitaxial relationship between the layer orientations is achieved. The pronounced (111) texture formed in the first Ta layer is reproduced by all subsequent three layers, and even some enhancement of its intensity is observed.

At -200 V (see Fig. 3, b), another mechanism of texture formation is observed. This includes the absence of dominance of the (111) orientation, as well as the vi-

olation of epitaxy. In the first and third Ta layers, the pole density of the (222) reflection is maximum, but still lower than at a voltage of -100 V. In this case, in the second and fourth W layers, the pole density of the (211) and (321) reflections is higher than reflection (222). The texture in the third tantalum and fourth tungsten layers completely reproduces the texture not of the previous layer, but the texture characteristic of the metal in the first and second layers. This indicates not a partial, but a complete absence of epitaxy. Partial violation of epitaxy would be accompanied by a gradual weakening of the intensity of all texture components with distance from the substrate. However, at $U_s = -200$ V, a texture is formed in each layer characteristic of this particular metal (see Fig. 3, b). This fundamentally distinguishes the texture formation mechanism at this voltage on the substrate from the mechanism typical for $U_s = -100$ V (see Fig. 3, a).

Figure 4 shows diffraction patterns of four-layer Ta/W/Ta/W coatings deposited on a flat substrate at voltages $U_s = 0, -50, -100$, and -200 V. In the absence of voltage on the substrate (Fig. 4, a) and at its value -50 V (Fig. 4, b) the (111) texture dominates, and at $U_s = -100$ V (Fig. 4, c) it is enhanced to such an extent that we can speak of its single-crystal character. At a voltage of -200 V, as on a cylindrical substrate, the (111) texture component is weakened. Of particular interest in this regard is the single-crystal texture shown in Fig. 4, c, which corresponds to the texture of the fourth W-layer.

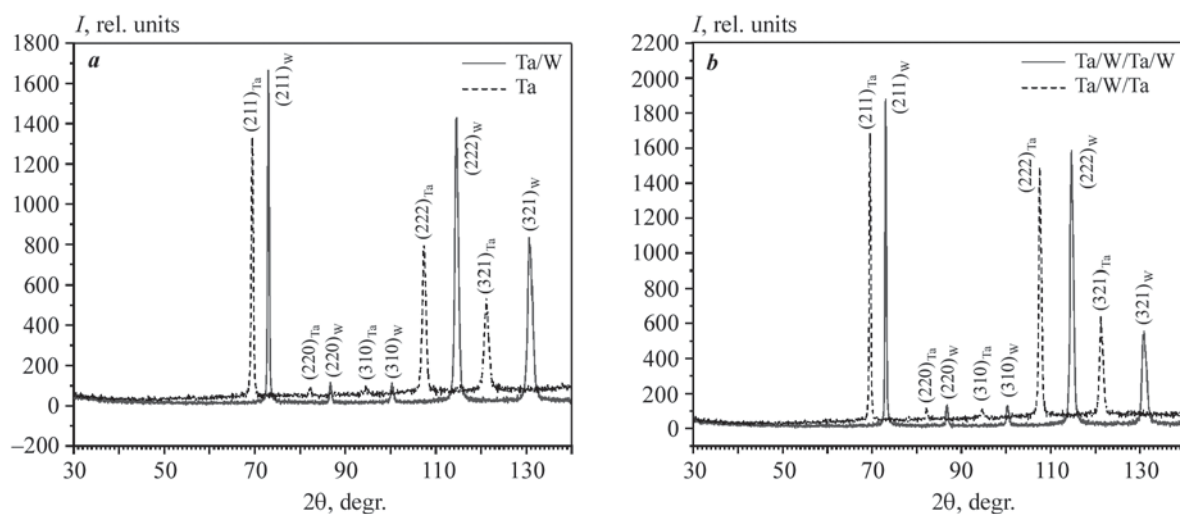


Fig. 1. Combined X-ray diffraction patterns of Ta, Ta/W (a) and Ta/W/Ta, Ta/W/Ta/W (b) magnetron coatings deposited on a cylindrical Cu substrate at $U_s = -100$ V

Рис. 1. Совмещенные дифрактограммы магнетронных покрытий Ta, Ta/W (a) и Ta/W/Ta, Ta/W/Ta/W (b) нанесенных на цилиндрическую Cu-подложку при напряжении $U_n = -100$ В

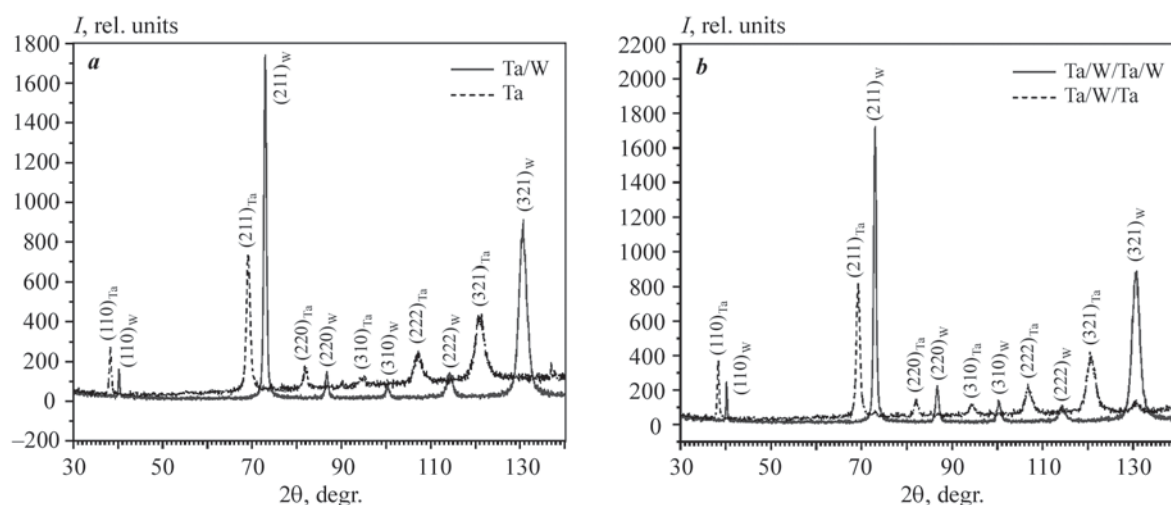


Fig. 2. Combined X-ray diffraction patterns of Ta, Ta/W (a) and Ta/W/Ta, Ta/W/Ta/W (b) magnetron coatings deposited on a cylindrical Cu substrate at $U_s = -200$ V

Рис. 2. Совмещенные дифрактограммы магнетронных покрытий Ta, Ta/W (a) и Ta/W/Ta, Ta/W/Ta/W (b), нанесенных на цилиндрическую Cu-подложку при напряжении $U_{\Pi} = -200$ В

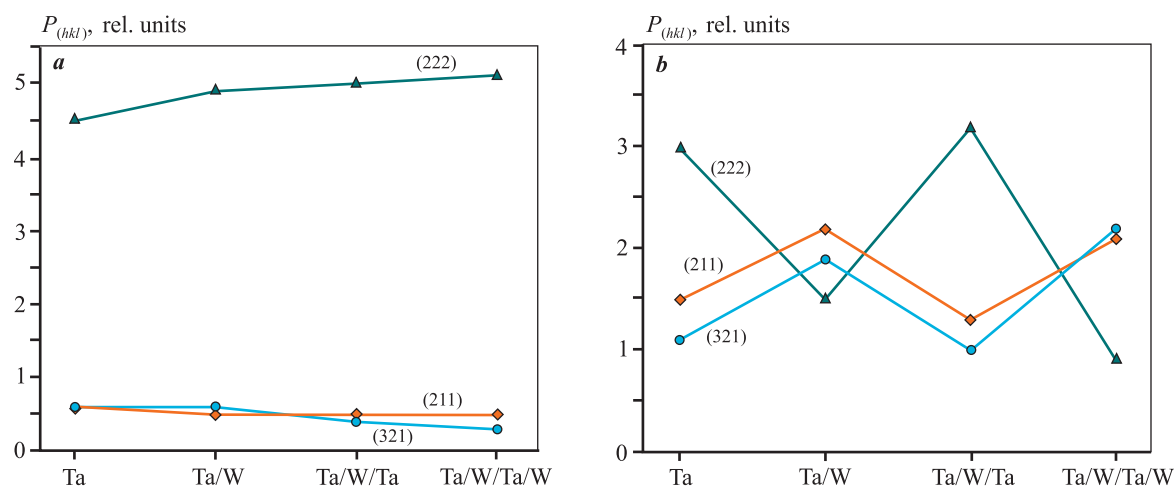


Fig. 3. Pole reflection densities (hkl) for layers of four-layer coatings deposited on a cylindrical Cu substrate at voltages $U_s = -100$ V (a) and -200 V (b)

Рис. 3. Полюсные плотности рефлексов (hkl) для слоев четырехслойных покрытий, нанесенных на цилиндрическую Cu-подложку при напряжениях $U_{\Pi} = -100$ В (a) и -200 В (b)

Figure 5, a shows reflection (222) for the outer W layer at tilt angles $\Psi = 0^\circ$, 5° , and 10° . When the deviation from the normal to the sample exceeds 10° , there are no grains with such a misorientation. The half-width of the texture maximum for the (222) reflection is $\sim 12^\circ$, corresponding to the misorientation angles of single-crystal nickel superalloys [20]. The diffraction pattern from the first Ta layer deposited at $U_s = -100$ V practically does not differ from that for the fourth W layer, which indicates that, as in the case of coatings on a cylindrical

substrate (see Fig. 3, a), at the mentioned voltage, an epitaxial correspondence of the orientations of successive layers is realized on it.

Figure 5, b shows reflections (222) for a single-layer Ta coating at angles $\Psi = 0^\circ$, 10° , and 15° , which demonstrate that there are no grains with such angle of misorientation when deviated from the normal to the sample by an angle of 15° . The half-width of the texture maximum for the (222) reflection for Ta layer is $\sim 14^\circ$, which, as in the case of a cylindrical substrate (see Fig. 3, a),

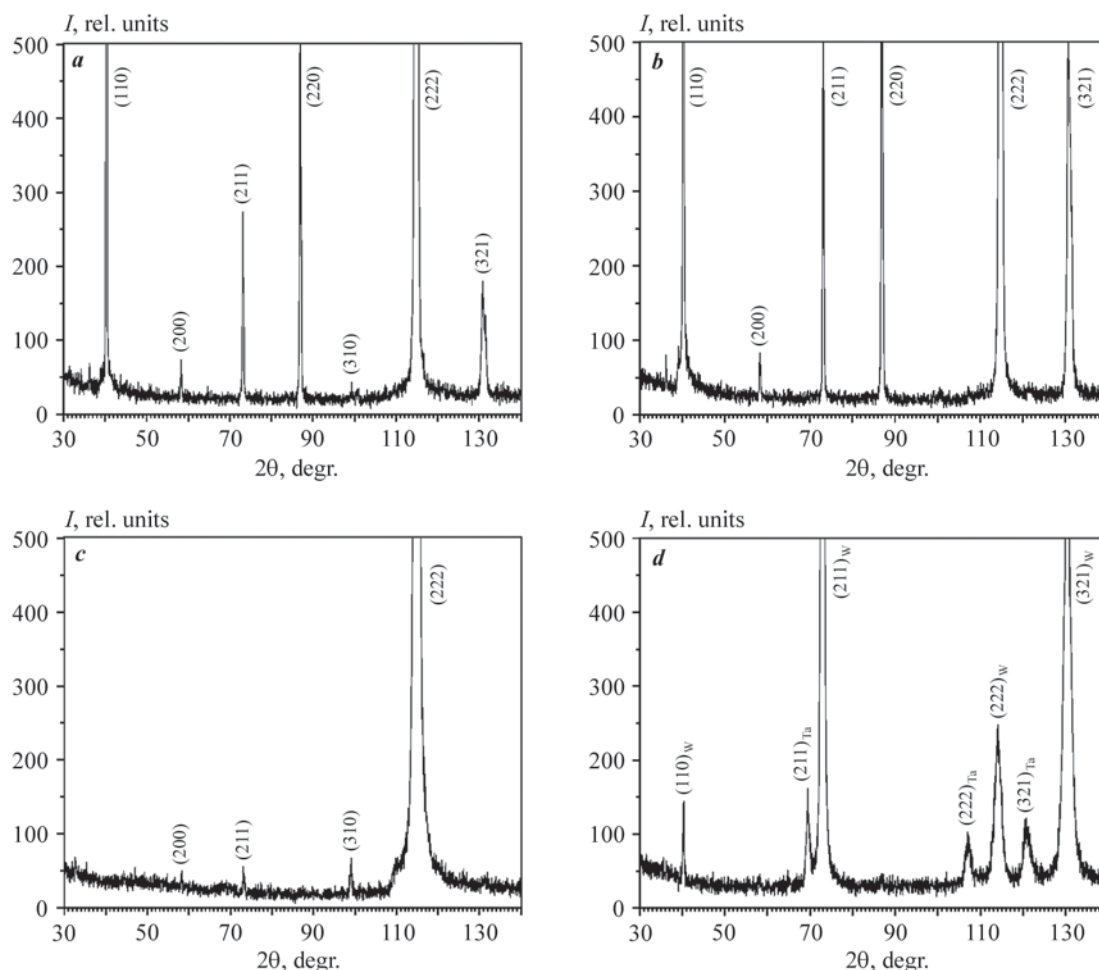


Fig. 4. X-ray diffraction patterns of outer W-layers of four-layer magnetron Ta/W/Ta/W coatings deposited at different substrate voltages

$U_s = 0$ (a), -50 V (b), -100 V (c) and -200 V (d)

Рис. 4. Дифрактограммы внешних W-слоев четырехслойных магнетронных покрытий Ta/W/Ta/W, нанесенных при различных напряжениях на подложке

$U_{\text{п}} = 0$ (a), -50 В (b), -100 В (c) и -200 В (d)

indicates an increase in the degree of texturization of the fourth layer compared to the first.

The importance of the result obtained is due to the fact that Ta has a “positive” elastic anisotropy, for which the maximum Young modulus (E_{max}) is located along the $\langle 111 \rangle$ direction of the Ta BCC lattice (Table 2). Therefore, the orientation of the coating plane parallel to the (111) crystallographic plane corresponds to the location of the direction with E_{max} and, accordingly, with the maximum value of the interatomic bond forces normal to the coating plane.

Thus, with a high degree of probability, high wear resistance should be expected in multilayer coatings with an external Ta layer. Tungsten is the only metal that does not have elastic anisotropy (Table 3), but it is possible

that the “single-crystal” orientation of W-layers will be useful for realizing other physicochemical properties, in relation to which this metal will have the necessary anisotropy.

Measuring residual stresses in four-layer coating

Our attempts to estimate the residual stresses for coatings deposited on cylindrical substrates failed. In essence this was the reason for applying coatings on a flat substrate. Problems also arose in estimating the residual stresses on the coatings, in which, at $U_s = -100$ V, a “single-crystal” texture was formed (see Fig. 5) for the outer layer of a four-layer Ta/W/Ta/W and a single-layer Ta coating.

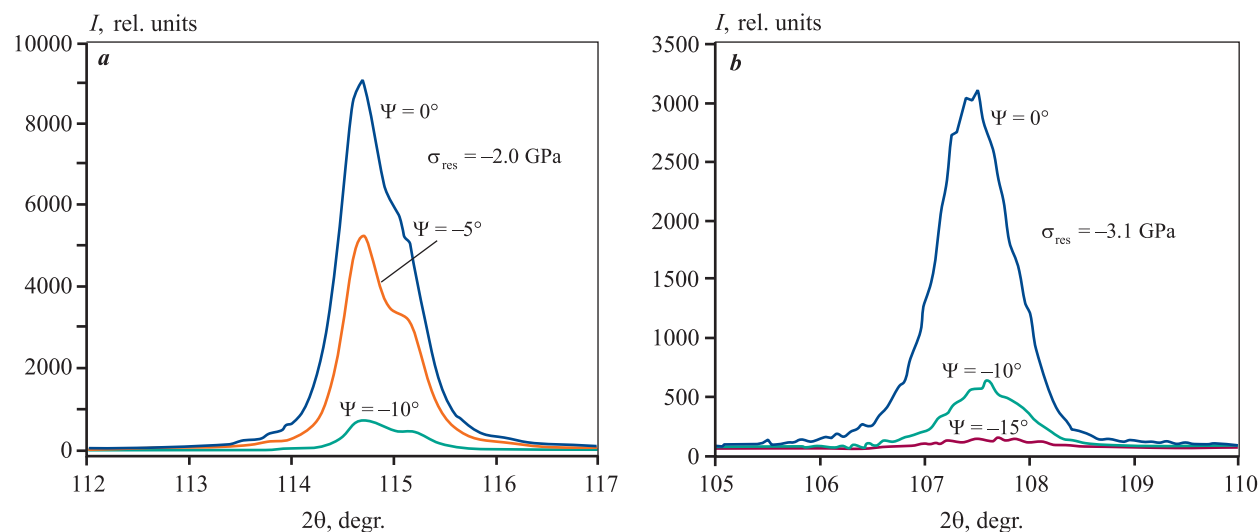


Fig. 5. Reflection (222) for pseudo-single-crystal magnetron coatings deposited at $U_s = -100$ V at various tilt angles Ψ
a – the outer W layer of the four-layer Ta/W/Ta/W coating; **b** – single-layer Ta-coating

Рис. 5. Рефлекс (222) для псевдомоноткристалльных магнетронных покрытий, нанесенных при $U_{\Pi} = -100$ В, при различных углах наклона Ψ

a – внешний W-слой четырехслойного Ta/W/Ta/W-покрытия; **b** – однослойное Ta-покрытие

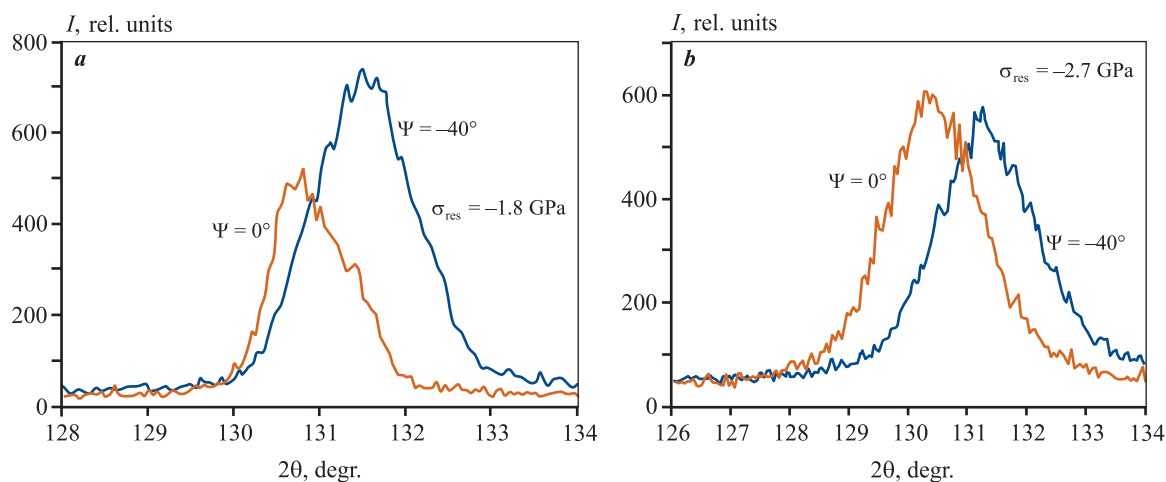


Fig. 6. Reflection (321) of the outer W-layer for four-layer Ta/W/Ta/W magnetron coatings deposited at $U_s = -50$ V (**a**) and -200 V (**b**) at tilt angles $\Psi = 0^\circ$ and -40°

Рис. 6. Рефлекс (321) внешнего W-слоя для четырехслойных Ta/W/Ta/W магнетронных покрытий, нанесенных при $U_{\Pi} = -50$ В (**a**) и -200 В (**b**) при углах наклона $\Psi = 0^\circ$ и -40°

The “ $\sin^2\Psi$ ” method provides for recording at tilt angles in the range from 0° to 40° – 60° . For single-crystal coatings, as can be seen from Fig. 5, the value of Ψ cannot exceed 10° , severely limiting the sensitivity of the method. Only the presence of ultrahigh stress values in both coatings made it possible to estimate the residual stresses for them. They amounted to -2.0 GPa for the

outer W layer in a four-layer coating and -3.1 GPa for a single-layer Ta coating.

Such a difference between the residual stresses can be attributed to two reasons. First, it is possible that the high stress value of a single-layer Ta-coating decreases in subsequent layers due to the mutual compensation of the thermal component of stresses when alternat-

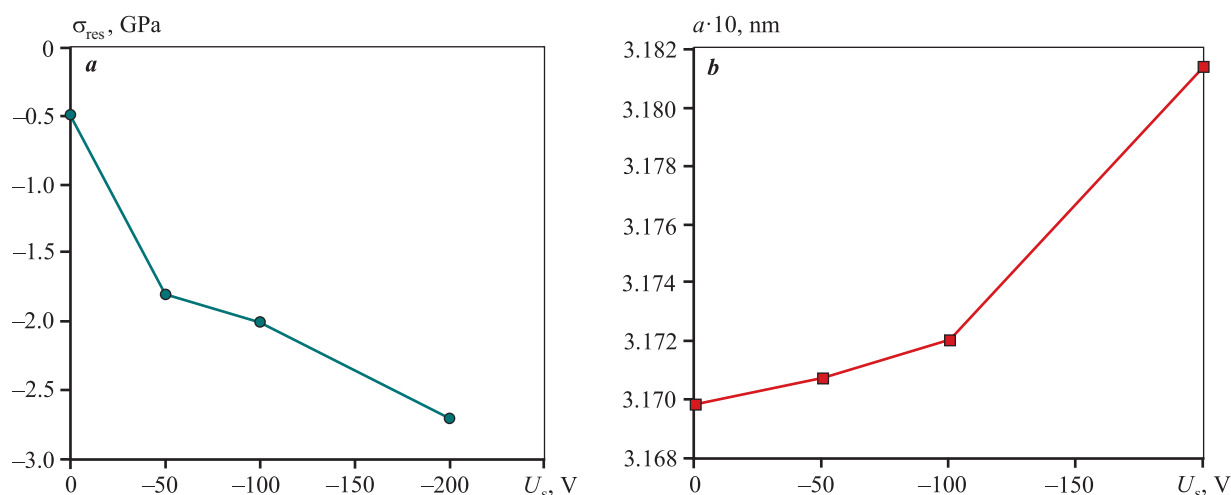


Fig. 7. Residual stresses (*a*) and lattice periods (*b*) of four-layer magnetron Ta/W/Ta/W coatings as a function of voltage on the substrate

Рис. 7. Зависимости остаточных напряжений (*a*) и периодов решетки (*b*) четырехслойных магнетронных покрытий Ta/W/Ta/W от напряжения на подложке

Table 2. Young's moduli for Ta and W $\langle uvw \rangle$ directions

Таблица 2. Значения модуля Юнга для $\langle uvw \rangle$ направлений Ta и W

$\langle uvw \rangle$	E , GPa	
	Ta	W
$\langle 110 \rangle$	193.4	409.8
$\langle 100 \rangle$	145.8	409.8
$\langle 211 \rangle$	193.4	409.8
$\langle 310 \rangle$	160.0	409.8
$\langle 111 \rangle$	217.1	409.8
$\langle 321 \rangle$	193.4	409.8

ing layers of refractory metals [21] differ in coefficient of thermal expansion (CTE) ($\alpha_W = 4.3 \cdot 10^{-6} \text{ K}^{-1}$ and $\alpha_{Ta} = 6.5 \cdot 10^{-6} \text{ K}^{-1}$). This leads to a decrease in stresses in the W-coating, which is the fourth layer. The second reason for such a difference in voltages may be related to the fact that the first Ta layer is deposited on a copper substrate, the CTE value of which ($\alpha_{Cu} = 16.6 \cdot 10^{-6} \text{ K}^{-1}$) differs from Ta by almost 5 times the difference of the W-layer from the preceding Ta layer.

For other coatings, the use of the “ $\sin^2\Psi$ ” method is not a problem. Figure 6 shows reflections (321) of the outer W-layer of four-layer coatings deposited at

voltages of -50 and -200 V. It can be seen that with a tilt of -40° , the intensity can be even higher than with symmetrical shooting ($\Psi = 0^\circ$). In general, the value of residual compressive stresses for four-layer coatings increases with increasing stress on the substrate (Fig. 7, *a*), due to which the value of the grating period also increases (Fig. 7, *b*).

Conclusions

1. The regularities of texture formation in a four-layer Ta/W/Ta/W coating obtained using a sputtering system of inverted magnetrons depend mainly on the voltage on the substrate, but differ for W and Ta layers. The latter is especially evident for coatings deposited at $U_s = -200$ V.

2. At a substrate voltage of -100 V, a special mechanism of texture formation operates, manifesting itself in the realization of an epitaxial relation between the layer orientations. In this case, for a cylindrical substrate, the strong texture (111) of the first Ta layer is reproduced by all subsequent three layers, while for a flat substrate, a single-crystal texture (111) is formed with a texture maximum width of 12° – 14° .

3. The presence of a single-crystal texture (111) of the Ta layer corresponds to the maximum Young modulus and, accordingly, the interatomic bond forces normal to the coating plane, suggesting that multilayer coatings with an external Ta layer have high tribological characteristics.

4. An increase in the voltage on a flat substrate from 0 to -200 V leads to an increase in residual compressive stresses from 0.5 to 2.7 GPa for a four-layer Ta/W/Ta/W coating.

5. In the first Ta-layer of the single-crystal coating, the residual stresses were -3.1 GPa, while in the fourth W-layer they were -2.0 GPa. This can be attributed to stress relaxation in the intermediate layers, as well as the fact that the difference in TCLE values between the first Ta layer and the Cu substrate is 5 times greater than the difference between the fourth W layer and the previous Ta layer.

References

- Dooho Choi, Bincheng Wang, Suk Chung, Xuan Liu, Amith Darbal, Adam Wise, Noel T. Nuhfer, Katayun Barmak. Phase, grain structure, stress, and resistivity of sputter-deposited tungsten films. *Journal of Vacuum Science & Technology: A*. 2011;29(5):051512. <http://dx.doi.org/10.1116/1.3622619>
- Pai Chi-Feng, Liu Luqiao, Li Y., Tseng H.W., Ralph D.C., Buhrman R.A. Spin transfer torque devices utilizing the giant spin hall effect of tungsten. *Applied Physics Letters*. 2012;101:122404. <http://dx.doi.org/10.1063/1.4753947>
- Vüllers F.T.N., Spolenak R. Alpha-vs. Beta-W nanocrystalline thin films: A comprehensive study of sputter parameters and resulting materials' properties. *Thin Solid Films*. 2015;577:26–34. <https://doi.org/10.1016/j.tsf.2015.01.030>
- Stelmakh V., Rinnerbauer V., Joannopoulos J.D., Soljačić M., Celanovic I., Senkevich J.J. Evolution of sputtered tungsten coatings at high temperature. *Journal of Vacuum Science & Technology: A*. 2013;31(6):061505. <http://dx.doi.org/10.1116/1.4817813>
- Chargui A., Beainou R.El., Mosset A., Euphrasie S., Pottin V., Vairac P., Martin N. Influence of thickness and sputtering pressure on electrical resistivity and elastic wave propagation in oriented columnar tungsten thin films. *Nanomaterials*. 2020;10(1):81. <https://doi.org/10.3390/nano10010081>
- Dutta N.J., Buzarbaruah N., Mohanty S.R. Damage studies on tungsten due to helium ion irradiation. *Journal of Nuclear Materials*. 2014;452(1-3):51–56. <http://dx.doi.org/10.1016/j.jnucmat.2014.04.032>
- Liudas Pranevicius. Magnetron-sputter deposition of W coatings for fusion applications. *Materials Science (Medžiagotyra)*. 2009;15(3):212–219.
- Esteve J., Zambrano G., Rincon C., Martinez E., Galindo H., Prieto P. Mechanical and tribological properties of tungsten carbide sputtered coatings. *Thin Solid Films*. 2000;373(1–2):282–286. [https://doi.org/10.1016/S0040-6090\(00\)01108-1](https://doi.org/10.1016/S0040-6090(00)01108-1)
- Nygren R.E., Raffray R., Whyte D., Urlickson M.A., Baldwin M., Snead L.L. Making tungsten work—ICFRM-14 session T26 paper 501. *Journal of Nuclear Materials*. 2011;417(1-3):451–456. <https://doi.org/10.1016/j.jnucmat.2010.12.289>
- Smid I., Akiba M., Vieider G., Plöchl L. Development of tungsten armor and bonding to copper for plasma-interactive components. *Journal of Nuclear Materials*. 1998;258-263(1):160–172. [https://doi.org/10.1016/S0022-3115\(98\)00358-4](https://doi.org/10.1016/S0022-3115(98)00358-4)
- Dias M., Mateus R., Catarino N., Franco N., Nunes D., Correia J. B., Carvalho P. A., Hanada K., Sarbu C., Alves E. Synergistic helium and deuterium blistering in tungsten–tantalum composites. *Journal of Nuclear Materials*. 2013;442(1-3):69–74. <https://doi.org/10.1016/j.jnucmat.2013.08.010>
- Colin J.J., Abadias G., Michel A., Jaouen C. On the origin of the metastable b-Ta phase stabilization in tantalum sputtered thin films. *Acta Materialia*. 2017;126:481–493. <https://doi.org/10.1016/j.actamat.2016.12.030>
- Gladczuk L., Patel A., Paur C.S., Sosnowski M. Tantalum films for protective coatings of steel. *Thin Solid Films*. 2004;467(1-2):150–157. <https://doi.org/10.1016/j.tsf.2004.04.041>
- Lee S.L., Windover D., Lub T.-M., Audino M. In situ phase evolution study in magnetron sputtered tantalum thin films. *Thin Solid Films*. 2002;420-421:287–294. [https://doi.org/10.1016/S0040-6090\(02\)00941-0](https://doi.org/10.1016/S0040-6090(02)00941-0)
- Lin J., Moore J.J., Sproul W.D., Lee S.L., Wang J. Effect of negative substrate bias on the structure and properties of Ta coatings deposited using modulated pulse power magnetron sputtering. *IEEE Transactions on Plasma Science*. 2010;38(11):3071–3078. <https://doi.org/10.1109/TPS.2010.2068316>
- Navid A.A., Hodge A.M. Nanostructured alpha and beta tantalum formation—Relationship between plasma parameters and microstructure. *Materials Science and Engineering: A*. 2012;536:49–56. <https://doi.org/10.1016/j.msea.2011.12.017>
- Myers S., Lin J., Souza R.M., Sproul W.D., Moore J.J. The β to α phase transition of tantalum coatings deposited by modulated pulsed power magnetron sputtering. *Surface & Coatings Technology*. 2014;214:38–45. <https://doi.org/10.1016/j.surfcoat.2012.10.061>
- Fritze S., Hans M., Riekehr L., Osinger B., Lewin E., Schneider J.M., Jansson U. Influence of carbon on microstructure and mechanical properties of magnetron sputtered TaW coatings. *Materials and Design*. 2020;196:109070. <https://doi.org/10.1016/j.matdes.2020.109070>
- Konuru S.L.K., Umasankar V., Sarma A. Deposition of tungsten–tantalum composite coating on RAFM steel

- by sputtering deposition process. *Fusion Engineering and Design*. 2020;160:111972.
<https://doi.org/10.1016/j.fusengdes.2020.111972>
20. Konuru S.L.K., Umasankar V., Sarma A. Development and characterisation of W and W–25%Ta composite coatings on steel material. *Journal of Surface Science and Technology*. 2020;36(3-4):103–108.
<https://doi.org/10.18311/jsst/2020/20109>
 21. Emmerlich J., Mráz S., Snyders R., Jiang K., Schneider J.M. The physical reason for the apparently low deposition rate during high-power pulsed magnetron sputtering. *Vacuum*. 2008;82(8):867–870.
<https://doi.org/10.1016/j.vacuum.2007.10.011>
 22. Thornton J.A., Hedgcock V.L. Tubular hollow cathode sputtering onto substrates of complex shape. *Journal of Vacuum Science & Technology*. 1975;12: 93–97.
<https://doi.org/10.1116/1.568631>
 23. Lozovan A.A., Lenkovets A.S., Ivanov N.A., Alexandrova S.S., Kubatina E.P. System of inverted magnetrons for the formation of multilayer composites on axisymmetric small-sized substrates. *Journal of Physics: Conference Series*. 2018;1121:012020.
<https://doi.org/10.1088/1742-6596/1121/1/012020>
 24. Lozovan A.A., Betsofen S.Ya., Lenkovets A.S., Grushin I.A., Labutin A.A., Pavlov Yu.S. Research of the effect of bias voltage on the morphology, structure and lattice spacings of the Nb coatings deposited by inverted magnetron. *Journal of Physics: Conference Series*. 2018;1121:012019.
<https://doi.org/10.1088/1742-6596/1121/1/012019>
 25. Shalin R.E., Svetlov I.L., Kachanov E.B., Toloraia V.N., Gavrilov O.S.. Single crystals of nickel heat-resistant alloys. Moscow: Mashinostroyeniye, 1997. 336 p. (In Russ.).
 Шалин Р.Е., Светлов И.Л., Качанов Е.Б., Толораия В.Н., Гаврилин О.С. Монокристаллы никелевых жаропрочных сплавов. М.: Машиностроение, 1997. 336 с.
 26. Betsofen S.Ya., Lozovan A.A., Lenkovets A.S., Labutin A.A., Grushin I.A. Texture and residual stresses in Mo, Nb, and Nb/Mo magnetron coatings. *Russian Metallurgy (Metally)*. 2021;(7):883–891.
<https://doi.org/10.1134/S0036029521070028>
 Бецофен С.Я., Лозован А.А., Ленковец А.С., Лабутин А.А., Грушин И.А. Исследование формирования текстуры и остаточных напряжений в магнетронных Мо-, Nb- и Nb/Mo-покрытиях. *Металлы*. 2021;4:87–98.

Information about the authors

Alexander A. Lozovan – Dr. Sci. (Eng.), Professor of the Department 1101, Moscow Aviation Institute (National Research University) (MAI (NRU)).

<http://orcid.org/0000-0001-9478-6793>

E-mail: loz-plasma@yandex.ru

Sergey Ya. Betsofen – Dr. Sci. (Eng.), Professor of the Department 1101, MAI (NRU).

<http://orcid.org/0000-0003-0931-2839>

E-mail: s.betsofen@gmail.com

Aleksandr S. Lenkovets – Cand. Sci. (Eng.), Senior Lecturer of the Department 1101, MAI (NRU).

<http://orcid.org/0009-0006-6271-2179>

E-mail: kompozitplasma@gmail.com

Alexey V. Shalin – Cand. Sci. (Eng.), Assistant Professor of the Department 1102, MAI (NRU).

<http://orcid.org/0009-0009-0660-7026>

E-mail: shalinaleks@yandex.ru

Nikolai A. Ivanov – Junior Research Scientist of the Department 1101, MAI (NRU).

<http://orcid.org/0009-0002-3513-8571>

E-mail: el8i7presley@gmail.com

Информация об авторах

Александр Александрович Лозован – д.т.н., профессор кафедры 1101, Московский авиационный институт (Национальный исследовательский университет) (МАИ (НИУ)).

<http://orcid.org/0000-0001-9478-6793>

E-mail: loz-plasma@yandex.ru

Сергей Яковлевич Бецофен – д.т.н., профессор кафедры 1101, МАИ (НИУ).

<http://orcid.org/0000-0003-0931-2839>

E-mail: s.betsofen@gmail.com

Александр Сергеевич Ленковец – к.т.н., ст. преподаватель кафедры 1101, МАИ (НИУ).

<http://orcid.org/0009-0006-6271-2179>

E-mail: kompozitplasma@gmail.com

Алексей Владимирович Шалин – к.т.н., доцент кафедры 1102, МАИ (НИУ).

<http://orcid.org/0009-0009-0660-7026>

E-mail: shalinaleks@yandex.ru

Николай Андреевич Иванов – мл. науч. сотрудник кафедры 1101, МАИ (НИУ).

<http://orcid.org/0009-0002-3513-8571>

E-mail: el8i7presley@gmail.com

Contribution of the authors

A.A. Lozovan – formulated the objectives of the study, conducted experiments, wrote the manuscript.

S.Ya. Betsofen – participated in the discussion of the results, wrote the manuscript.

A.S. Lenkovets – conducted experiments.

A.V. Shalin – conducted X-ray phase analysis.

N.A. Ivanov – prepared initial samples, conducted experiments, participated in the discussion of the results.

Вклад авторов

А.А. Лозован – определение цели работы, участие в обсуждении результатов, написание текста статьи.

С.Я. Бецофен – участие в обсуждении результатов, написание текста статьи.

А.С. Ленковец – проведение экспериментов.

А.В. Шалин – проведение рентгенофазового анализа.

Н.А. Иванов – подготовка исходных образцов, проведение экспериментов, участие в обсуждении результатов.

The article was submitted 22.05.2023, revised 25.05.2023, accepted for publication 29.05.2023

Статья поступила в редакцию 22.05.2023, доработана 25.05.2023, подписана в печать 29.05.2023